

# ILMENITE PROCESSING IN THERMAL PLASMA DURING ELECTRIC DISCHARGE MECHANICAL MILLING

Damon Bishop, Brian Monaghan & Andrzej Calka  
University of Wollongong, Australia

## ABSTRACT

*The novel and advanced Electric Discharge Assisted Mechanical Milling (EDAMM) technique has been evaluated for use in the mineral processing of natural ilmenite concentrates (NIC). The authors have demonstrated EDAMM is an effective tool for inducing rapid reaction rates in oxide-gas systems, though work thus far has concentrated on synthesis reactions of high purity laboratory grade materials such as  $Fe_2O_3$ ,  $PbS$  and  $Sb_2O_3$ . Using NIC as the primary reagent, phase changes during thermal decomposition and oxidation of ilmenite concentrate induced by EDAMM were established. Experiments were carried out in  $CO_2$ ,  $N_2$ ,  $Ar$ ,  $O_2$  and air. Products were characterized by XRD and SEM. The results of this investigation demonstrate that thermal decomposition of the pseudorutile component of ilmenite concentrate occurs during EDAMM in less than 10 seconds and that oxidation of the ilmenite component occurs during EDAMM in less than 2 minutes in oxidising atmospheres.*

## INTRODUCTION

There is a constant drive to improve the efficiency of extraction metallurgy processes. These efficiency measures fall into two categories, incremental improvements of extant processes or new processes offering different process route possibilities. Electric discharge assisted mechanical milling (EDAMM) is a relatively new laboratory process that combines reactive ball milling with plasma arc processing to effect both the reaction of a material and refine its size and morphology. [1]. Though as yet only demonstrated on small laboratory scale experiments; if it can be scaled up, this new process offers potential improvement in terms of productivity, energy consumption and lessening of environmental impact over a number of current processes used to consolidate, refine and reduce ores.

The EDAMM process has been demonstrated as an effective tool for inducing rapid reaction rates in solid-solid systems and solid-gas systems [2, 3, 4]. Control over the degree of reaction and particle morphology has also been demonstrated. Work conducted thus far has concentrated on synthesis reactions. Partial reduction has only been demonstrated for haematite ( $\text{Fe}_2\text{O}_3$ ) [5]. In addition, all the materials studied up to now have been high purity, laboratory grade powders such as  $\text{Fe}_2\text{O}_3$ , PbS and  $\text{Sb}_2\text{O}_3$ . With this in mind, it is possible that phase changes induced by EDAMM in industrial grade materials could represent an intermediate step, or even the primary step in a metals extraction route. It is unknown how the presence of gangue or waste minerals present in commercial grade minerals will impact the ability of EDAMM to induce phase changes.

## METHODOLOGY

To assess the effects of using industrial as opposed to laboratory grade material in the EDAMM process natural ilmenite concentrates (NIC) were chosen as the sample material for this investigation. A schematic of the EDAMM is given in Figure 1. In an EDAMM mill a vibrating base produces a milling mode involving repeated impact of a hardened curved rod end on particles placed in a vibrating hemispherical container under a controlled electrical discharge in a controlled atmosphere. Electric discharges occur in the gap between the vibrating mill base, the powder particles and the rod. These electric discharges result in hot plasma formation near ilmenite powder particles. The mill uses a power supply capable of generating 1 kV, impulses within the mA and kHz range.

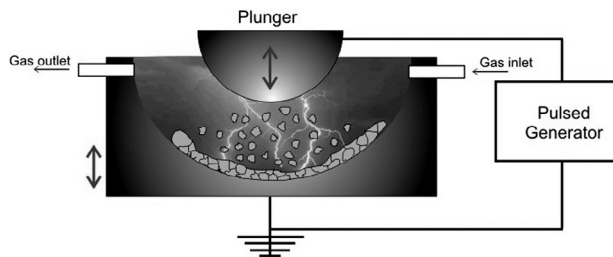


Figure 1: A schematic of the Electric Discharge Assisted Mechanical Milling (EDAMM) technique

Experiments were conducted in atmospheres of  $\text{N}_2$ ,  $\text{CO}_2$ , Ar,  $\text{O}_2$  and air and changes in phase, particle size and morphology were observed and characterized using XRD and SEM techniques. In all experiments a milling time up to 10 min was used. Less than 1g sample masses were used in all experiments. X-ray diffraction (XRD) analysis was performed using a Phillips PW1730 diffractometer with a graphite monochromator and Cu K $\alpha$  radiation. Phase identification was carried out using the International Centre for

Diffraction Data (JCPDS-ICDD 2000) powder diffraction files. The morphology of the powders was observed by a Leica 440 Stereoscan SEM. This SEM is equipped with an Oxford Instruments ISIS EDS system which was used to examine the composition of the powders.

## RESULTS AND DISCUSSION

### Decomposition of NIC

NICs are obtained by magnetic separation from mineral sand deposits. This concentrate is primarily an iron-titanium oxide. Two principal phases found in NIC are ilmenite ( $\text{FeTiO}_3$ ) and pseudorutile ( $\text{Fe}_2\text{Ti}_3\text{O}_9$ ) [6].

The NIC was subjected to EDAMM in  $\text{CO}_2$ ,  $\text{N}_2$  and Ar atmospheres for 10 minutes. Milling times and phases identified by XRD for the starting powder and EDAMM products are summarised in Table 1 and XRD curves are given in Figure 2.

Table 1: Phases identified by XRD for NIC decomposition experiments

Sample	Milling time (min.)	Atmosphere	Phases identified
Starting powder			Ilmenite, Pseudorutile
#1	10	$\text{CO}_2$	Pseudobrookite, Ilmenite
#2	10	$\text{N}_2$	Pseudobrookite, Ilmenite
#3	10	Ar	Pseudobrookite, Ilmenite

Analysis of the XRD curves in Figure 2 confirmed the presence of both ilmenite ( $\text{FeTiO}_3$ ) and pseudorutile ( $\text{Fe}_2\text{Ti}_3\text{O}_9$ ) in the starting NIC. Further, the XRD results of EDAMM for 10 minutes in all three gases show that the ilmenite phase of the original NIC has been retained. However, the pseudorutile has been eliminated and replaced with ferric pseudobrookite ( $\text{Fe}_2\text{TiO}_5$ ) another iron-titanium oxide phase.

These phase analyses confirm that EDAMM processing of NIC in  $\text{CO}_2$ ,  $\text{N}_2$  and Ar atmospheres induces decomposition of pseudorutile ( $\text{Fe}_2\text{Ti}_3\text{O}_9$ ). Decomposition of pseudorutile can be represented by Equation 1. From Equation 1 the expected decomposition products of pseudorutile are ferric pseudobrookite ( $\text{Fe}_2\text{TiO}_5$ ) and rutile ( $\text{TiO}_2$ ).



No rutile was observed in the XRD analysis. There is much still unknown about the EDAMM process. In particular, the temperature and temperature gradients that the materials experience during the processing and key gas reaction species produced are expected to play a critical role in the reaction scheme. This makes comparison of EDAMM process with other experimental techniques problematic. In a conventional sintering study under argon using similar materials Zhang *et al.* [6], observed that rutile peaks disappeared when ilmenite was sintered at  $1400^\circ\text{C}$  for 2 hours. Their explanation of this was that at these high temperatures, rutile is taken into a solid solution with ferric pseudobrookite. This may also be true for the rutile in the EDAMM experiments and that the cooling of the reacted NIC in the EDAMM was sufficient to freeze in the structure. On the basis of product formed only, comparison of Zhang *et al.* [6] results via conventional heat treatment with those during EDAMM processing of NIC indicates that a condition equivalent conventional processing at  $1400^\circ\text{C}$  has been exceeded for the case of EDAMM. It should be noted the authors are not stating that this is the EDAMM process temperature or even a local NIC surface

temperature during EDAMM processing, as the complexity of the reaction system studied and mechanisms operative during EDMM have not yet been fully delineated.

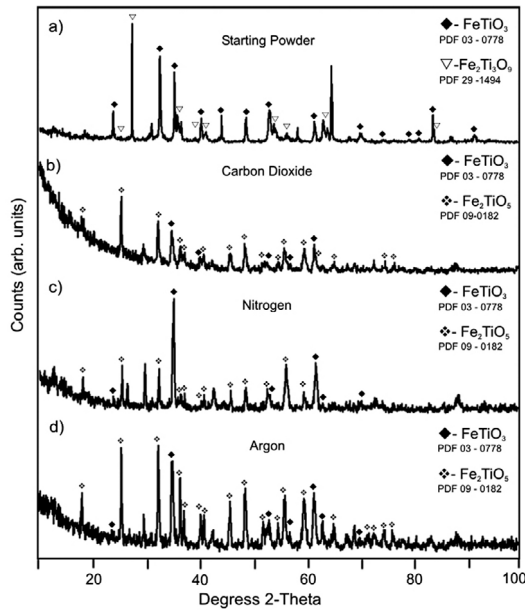


Figure 2: XRD patterns of NIC before and after milling for 10 minutes using EDAMM in various atmospheres where (a) is the NIC starting powder, (b) milled in  $\text{CO}_2$  gas, (c) milled in  $\text{N}_2$  gas and (d) Milled in Ar gas

From the results presented it can be stated that EDAMM processing of NIC in  $\text{CO}_2$ ,  $\text{N}_2$  and Ar atmospheres induces thermal decomposition of the pseudorutile component in under 10 minutes and that the ilmenite component is retained.

In Figure 3, a SEM secondary electron image of the starting NIC material shows that the concentrate has a smooth surface. In Figure 4, a SEM secondary electron image of the NIC sample after EDAMM processing under argon for 10 minutes is given. In this Figure it can be seen that after processing the NIC sample has a much more irregular shape. Close inspection of this sample at higher magnifications shows what could be described as a stepped or layered edge. The surface of the examined particle shows patches of smooth areas as well as jagged areas which appear to be an agglomeration of smaller particles or crystals.

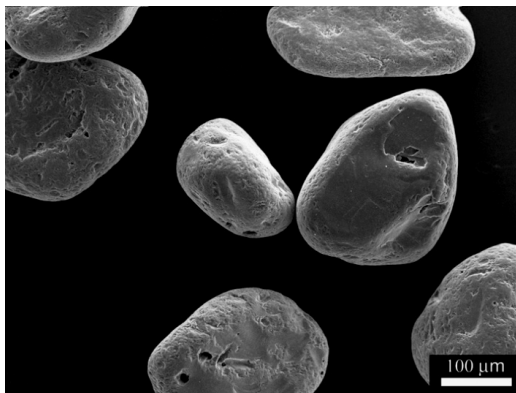


Figure 3: SEM secondary electron image showing the NIC starting powder. The scale bar is 100  $\mu\text{m}$

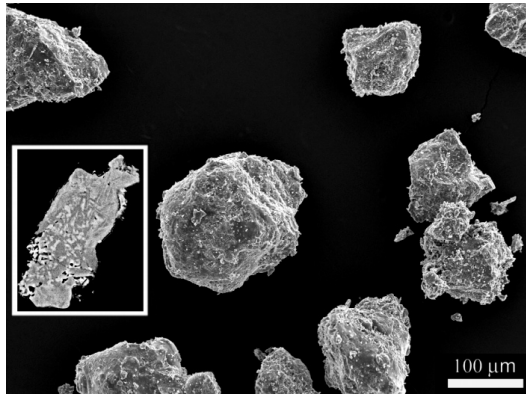


Figure 4: SEM secondary electron image showing the NIC sample after reaction in EDAMM for 10 minutes under Ar gas. The scale bar is 100  $\mu\text{m}$

There appears to be a marginal size reduction due to the EDAMM processing. The starting NIC sample has a typical particle diameter of about 200  $\mu\text{m}$ . After EDAMM processing in argon the typical particle diameter was approximately 150  $\mu\text{m}$ . There are also some smaller particles (<10  $\mu\text{m}$ ). These small particles appear both on their own and adhered to the surface of the larger particles. It is likely they have formed by chipping from the larger, irregular particles due to the mechanical milling action.

Inspection of the SEM image of a cross sectioned particle subjected to EDAMM processing in argon for 10 minutes (Figure 4 inset) shows atomic number contrast indicating that at least two phases are present in the particles. This is consistent with the two phases, ilmenite and ferric pseudobrookite, identified by XRD analysis.

### Oxidation of NIC

In these experiments the NIC was subjected to EDAMM processing in air and oxygen atmospheres for 10 minutes. Phases identified by XRD for the starting powder and EDAMM process products are summarised in Table 2. Labelled XRD patterns for NIC subjected to EDAMM in oxidising atmospheres are shown in Figure 5.

As before the XRD results confirm the presence of both ilmenite ( $\text{FeTiO}_3$ ) and pseudorutile ( $\text{Fe}_2\text{Ti}_3\text{O}_9$ ) in the NIC starting powder. Samples after EDAMM processing in an atmosphere of oxygen or air developed the iron-titanium oxide, ferric pseudobrookite ( $\text{Fe}_2\text{TiO}_5$ ) phase. The ilmenite and pseudorutile starting phases were both eliminated during EDAMM processing.

Table 2: Phases identified by XRD for NIC oxidation experiments

Sample	Milling time (min.)	Atmosphere	Phases identified
Starting powder			Ilmenite, Pseudorutile
#4	10	$\text{O}_2$	Pseudobrookite
#5	10	Air	Pseudobrookite

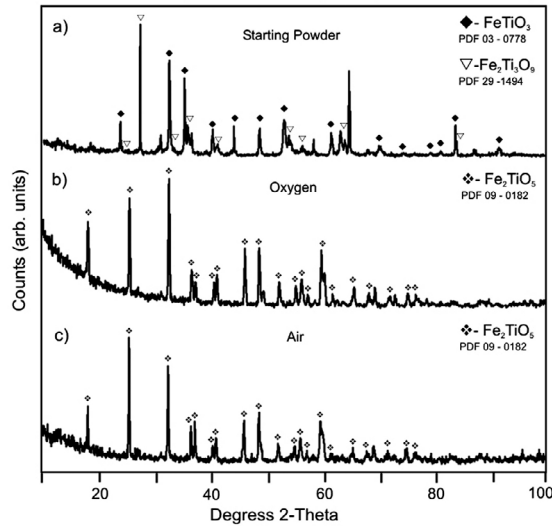


Figure 5: XRD patterns of NIC before and after milling for 10 minutes using EDAMM in oxidising atmospheres where (a) is the NIC starting powder, (b) milled in  $O_2$  gas and (c) milled in air

The XRD results show that EDAMM processing of NIC in an atmosphere of oxygen or air induces decomposition of the pseudorutile ( $Fe_2Ti_3O_9$ ) phase and complete oxidation of the ilmenite ( $FeTiO_3$ ) phase in less than 10 minutes. Equation 2 can be used to represent the decomposition reaction of pseudorutile. From equation 2 it can be seen that the expected products of decomposition of pseudorutile are ferric pseudobrookite ( $Fe_2TiO_5$ ) and rutile ( $TiO_2$ ).



Likewise, the expected products from oxidation of ilmenite are ferric pseudobrookite and rutile. The overall reaction is shown in Equation 3.



The absence of rutile from any of the XRD patterns in Figure 5 is consistent with the work by Zhang *et al.* [6], who found that rutile peak intensity diminished with time under oxidising conditions at  $1400^\circ C$ , and similar to what was observed and discussed when processing in  $CO_2$ ,  $N_2$  and Ar atmospheres. See Decomposition of NIC section for caveats and explanation.

In Figure 6 a SEM secondary electron image of the NIC sample after EDAMM processing in air for 10 minutes is given. From this Figure it can be seen that the EDAMM and oxidised sample has a much more irregular shape than the starting NIC. Close inspection of this sample at  $2500\times$  shows that the morphology of the oxidized product consists of acicular or needle-like crystals. This is consistent with Amethyst Galleries (2007) description of the crystal habit of ferric pseudobrookite as *including small acicular or thin prismatic crystals aggregated together as sprays of only a few individuals*.

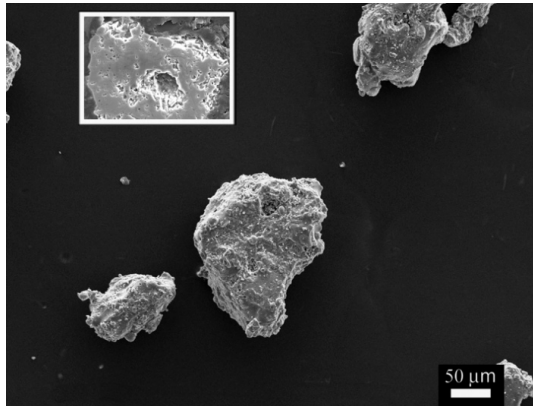


Figure 6: SEM secondary electron image showing the ilmenite sample after reaction in EDAMM for 10 minutes in air. Inset shows cross sectioned particle image. The scale bar is 50  $\mu\text{m}$

The size of the particles has been reduced after EDAMM processing. The starting NIC sample has a typical particle diameter of about 200  $\mu\text{m}$  whereas the sample after EDAMM processing in air has a typical particle diameter of about 100  $\mu\text{m}$ . As before when EDAMM processing under argon some much smaller particles (<10  $\mu\text{m}$ ) can also be found and a similar milling mechanism, as given in the Decomposition of NIC section, is thought to be responsible for the small particles.

Inspection of the SEM images of cross sectioned powders (Figure 6 inset) does not reveal any atomic number contrast which indicates that these are single phase particles with little or no segregation of elements.

From the above results of the EDAMM processing of NIC in air and  $\text{O}_2$  gas atmospheres it can be concluded that pseudobrookite component has undergone complete decomposition and the oxidation of the ilmenite component is complete in under 10 minutes.

### Effect of EDAMM Processing Time on Oxidation of NIC

From the forgoing results it was not possible to delineate the full reaction sequence of the oxidation of NIC. Zhang *et al.* [6], identified that haematite ( $\text{Fe}_2\text{O}_3$ ) was an intermediate reaction product of the oxidation of ilmenite. This phase was not found in the XRD analysis of the EDAMM processing 10 minutes in air or  $\text{O}_2$ . In order to assess the reaction sequence in the EDAMM process a series of experiment were carried out whereby the processing time was varied from 10 seconds to 10 minutes under an air atmosphere. The results of phase analysis and XRD curves are given in Table 3 and Figures 7 and 8.

Table 3: Phases identified by XRD for NIC oxidation in air experiments at various times

Sample	Milling time	Phases identified
Starting powder		Ilmenite Pseudobrookite
#6	10 seconds	Ilmenite, Pseudobrookite, Rutile
#7	30 seconds	Ilmenite, Pseudobrookite, Rutile
#8	1 minute	Ilmenite, Pseudobrookite, Rutile
#9	2 minutes	Pseudobrookite, Rutile
#10	5 minutes	Pseudobrookite
#11	10 minutes	Pseudobrookite

After 10 seconds, the product phases ferric pseudobrookite ( $\text{Fe}_2\text{TiO}_5$ ) and rutile ( $\text{TiO}_2$ ) have begun to appear. Ferric pseudobrookite is retained right through the entire EDAMM time series however rutile disappears between 2 minutes and 5 minutes of EDAMM duration. The XRD results (Figure 7 and 8) show that subjecting NIC to EDAMM processing in air induces decomposition of the pseudorutile ( $\text{Fe}_2\text{Ti}_3\text{O}_9$ ) component and oxidation of the ilmenite ( $\text{FeTiO}_3$ ) component in less than 2 minutes. The pseudorutile component could not be found after just 10 seconds of EDAMM processing. Indicating its decomposition was rapid. Some ilmenite was retained up to 1 minute of EDAMM processing. As discussed previously, the expected products of thermal decomposition of pseudorutile are ferric pseudobrookite and rutile. Likewise, the expected products from oxidation of ilmenite are also ferric pseudobrookite and rutile.

Both of ferric pseudobrookite and rutile product phases can be seen from 10 seconds of EDAMM processing, however the rutile phase disappears from the XRD patterns after 2 minutes of EDAMM. See previous discussion in the Decomposition of NIC section for a possible explanation of the absence of rutile from the XRD analysis.

It was thought that haematite ( $\text{Fe}_2\text{O}_3$ ) would form as an intermediate reaction product and be identified in the shorter milling durations. This was not the case. It was not clear if this was because haematite only existed for a short time in between the EDAMM processing steps or due to the different nature of the experimental approaches used in this study, as compared to Zhang *et al.* [6], resulted in a different reaction scheme occurring.

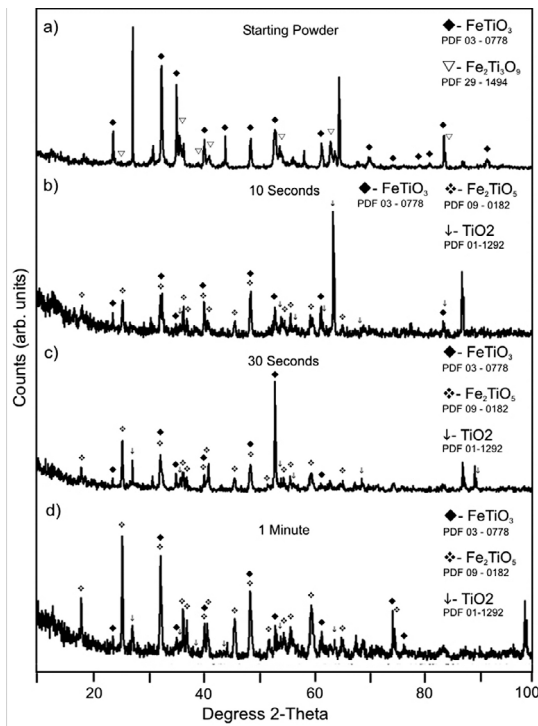


Figure 7: XRD patterns of NIC before and after EDAMM processing for times up to 10 minutes in an air atmosphere

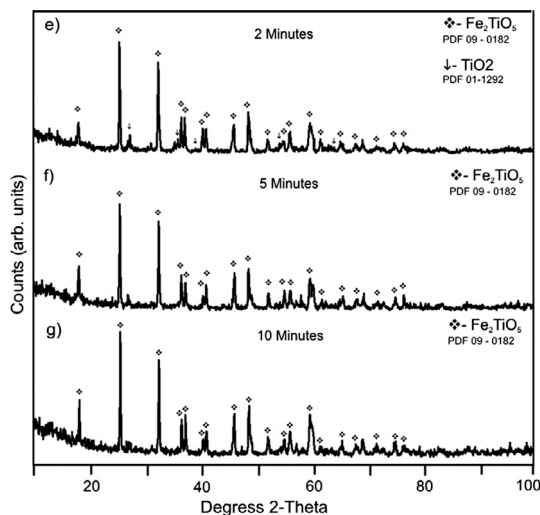


Figure 8: XRD patterns of NIC before and after EDAMM processing for times up to 10 minutes in an air atmosphere

## CONCLUSIONS

NIC has been subjected to EDAMM processing in  $\text{CO}_2$ ,  $\text{N}_2$ , Ar,  $\text{O}_2$  and air atmospheres in this study. It has been shown that processing in the  $\text{CO}_2$ ,  $\text{N}_2$ , Ar atmospheres the pseudorutile phase is decomposed to ferric pseudobrookite whilst the ilmenite phase remains unreacted. It has also been shown that in  $\text{O}_2$  and air atmospheres, the pseudorutile phase is again decomposed to ferric pseudobrookite, whilst the ilmenite phase is oxidised to ferric pseudobrookite.

Conducting EDAMM experiments on NIC over a range of durations demonstrated that during EDAMM processing, the pseudorutile phase is decomposed in less than 10 seconds, whilst the ilmenite phase is completely oxidised in less than 2 minutes. XRD results indicate that rutile, which is a product of these reactions is likely to have been taken into solid solution with ferric pseudobrookite during EDAMM. If this can be confirmed it indicates that conditions in the EDAMM reaction zone are equivalent to a temperature of at least  $1400^\circ\text{C}$ . As stated previously the authors are not stating that EDAMM process temperature or even a local NIC surface temperature during EDAMM processing is in excess of  $1400^\circ\text{C}$ , as the complexity of the reaction system studied has not yet been fully delineated but that reactions normally associated with high temperatures are possible in EDAMM processing.

## REFERENCES

- Calka, A. & Wexler, D. (2002). *Nature*, Vol. 419, pp. 147-151. [1]
- Needham S. A., Calka, A., Wang, G. X., Germanas, P. & Liu, H. K. (2006). *Journal of Materials Chemistry*. Vol. 16, No. 46, pp. 4488 - 4493. [2]
- Needham, S. A., Calka, A., Wang, G. X., Mosbah, A. & Liu, H. K. (2006). *Electrochemistry Communication*. 8, pp. 434 - 438. [3]

**Calka, A. & Oleszak, D.** (2007). *Journal of Metals and Compounds*, 440 No. 1-2 (2007), pp. 346 - 348. [4]

**Wexler, D. & Calka, A. & Dunne, D. P.** (2005). *Journal of Metastable and Nanocrystalline Materials*. 26, pp. 16 - 21. [5]

**Zhang, G. & Ostrovski, O.** (2002). *International Journal of Mineral Processing*. Vol. 424, pp. 201- 218. [6]